VIBRATION ANALYSIS OF A ROTOR SYSTEM SUPPORTED BY NONLINEAR HYDRODYNAMIC BEARINGS

PHÂN TÍCH DAO ĐỘNG PHI TUYẾN CỦA HỆ ROTOR - Ổ TRỤC THỦY LỰC

Van-Thanh Ngo

Faculty of Mechanical-Automotive and Civil Engineering, Electric Power University

Email: thanhnv@epu.edu.vn

ABSTRACT

In practice, linear analysis is often employed to calculate and predict physical phenomena during the vibration of rotor – bearing systems. However, in certain cases, nonlinear analysis is necessary to ensure the required level of accuracy. This paper conducts an analysis and comparison of a rotor system mounted on hydrodynamic bearings under both linear and nonlinear conditions. The nonlinear bearing force is modeled based on short bearing theory, incorporating the effects of oil film viscosity and bearing clearance. The results emphasize the critical importance of accounting for bearing force nonlinearity in accurately predicting the rotor's dynamic response.

Keywords: *Nonlinear analysis; Hydrodynamic bearings; Bearing force; Rotor dynamic.*

TÓM TẮT

Trong thực tế, phân tích tuyến tính thường được sử dụng để tính toán, dự đoán các hiện tượng vật lí trong quá trình dao động của hệ rotor ổ trục. Tuy nhiên, trong một số trường hợp cần sử dụng bài toán phi tuyến để phân tích nhằm đảm bảo độ chính xác cần thiết. Bài báo này tiến hành phân tích và so sánh hệ rotor lắp đặt trên ổ trục thủy lực trong hai trường hợp tuyến tính và phi tuyến. Lực từ ổ trục phi tuyến được xây dựng dựa trên lý thuyết ổ ngắn, có xét đến độ nhớt của màng dầu và khe hở ổ. Kết quả nhấn mạnh vai trò quan trọng của việc xét đến tính phi tuyến của lực ổ trục trong dự đoán chính xác đáp ứng động học của rotor.

Từ khóa: *Phân tích phi tuyến; Ổ trục thủy lực; Lực ổ trục; Động lực học rotor.*

1. INTRODUCTION

Rotor-bearing systems are fundamental components in a wide range of mechanical equipment, including turbines, compressors, generators, and high-speed machinery. Accurate prediction of their dynamic behavior is critical to ensure operational stability, safety, and efficiency. Traditional linear models of rotor dynamics have provided substantial insight; however, nonlinear effects arising from hydrodynamic bearings, material properties, and large amplitude vibrations can significantly alter system response, especially at high rotational speeds [1, 2].

Among these nonlinear sources, hydrodynamic journal bearings play a pivotal role due to the complex fluid-structure interactions between the rotating shaft and the surrounding oil film. The nonlinearity stems from the pressure distribution in the thin lubricant film, which depends nonlinearly on shaft eccentricity and velocity. This leads to phenomena such as sub-synchronous vibrations, bifurcations, and even chaotic motion under certain conditions [3, 4]. Consequently, accurately modeling and analyzing these nonlinearities are essential for modern rotor dynamics studies.

Recent advances in computational techniques and finite element modeling have enabled detailed investigations into nonlinear rotor-bearing systems [5, 6]. Particularly, the use of Timoshenko beam elements allows for the inclusion of shear deformation and rotary inertia effects, which are crucial for short and thick shafts. Moreover, the integration of nonlinear bearing forces into time-domain simulations has provided deeper understanding of transient responses and stability boundaries under various operational conditions [7].

Previous research efforts have highlighted that nonlinear oil-film forces can cause significant mode splitting, amplitude-dependent natural frequencies, and reduction in critical speeds [8]. Furthermore, experimental studies and numerical simulations have demonstrated the importance of considering bearing-induced damping and stiffness variations, which directly affect rotor stability margins [9, 10].

In this study, a detailed nonlinear dynamic analysis of a rotor system supported by hydrodynamic bearings is conducted. The shaft is modeled using six Timoshenko beam elements, while the bearings are represented with nonlinear force-displacement and force-velocity relationships based on short-bearing theory. The system's response is investigated at stationary (0 rpm) and operational (4,000 rpm) conditions. Modal analysis is performed to determine the natural frequencies and mode shapes, and time-domain simulations are carried out to capture nonlinear dynamic phenomena. This work aims to provide further insight into the complex dynamic behavior of rotors supported by nonlinear fluid film bearings, offering valuable guidance for the design and operation of rotating machinery.

2. SYSTEM CONFIGURATION

2.1. Geometrical and Material Properties

The rotor system comprises a steel shaft with two disks and is supported by hydrodynamic journal bearings as Figure 1. A 1.5m long shaft, has a diameter of 0.05m discretized into six Timoshenko beam elements, allowing for the inclusion of shear deformation and rotary inertia effects. The disks are keyed to the shaft at 0.4 and 1.2m from one end. The left disk is ☞

0.08m thick with a diameter of 0.3 m; the right disk is 0.07m thick with a diameter of 0.35m. Each node possesses four degrees of freedom: two translational and two rotational. Disks are modeled as lumped masses with appropriate inertias at their respective locations. For both the shaft and the disk, material are steel with $\rho = 7\,180$ kg/m^3; $E = 2.10^{11}$ GN/m^2 and $G = 81.2$ GN/m^2.

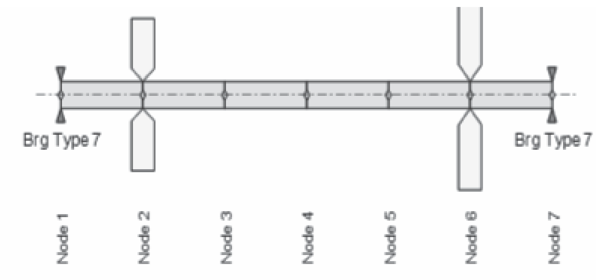

Figure 1. FEM mesh of the shaft

2.2. Bearings Modeling

A nonlinear-bearing model for a short, oil-film journal bearing as shown in Figure 2. The nonlinear relationship between bearing forces and journal displacement displacements u and v as:

$$\begin{Bmatrix} f_x \\ f_y \end{Bmatrix} = \eta\Omega L\left(\frac{D}{2c}\right)^2\left(\frac{L}{D}\right)^2\begin{Bmatrix} \hat{f}_x \\ \hat{f}_y \end{Bmatrix} \quad (1)$$

$$\begin{Bmatrix} \hat{f}_x \\ \hat{f}_y \end{Bmatrix} = -\frac{c\sqrt{(u\Omega-2\dot{v})^2+(v\Omega+2\dot{u})^2}}{\Omega(c^2-u^2-v^2)}\begin{Bmatrix} 3V\left(\frac{u}{c}\right) - G\sin\alpha - 2S\cos\alpha \\ V\left(\frac{v}{c}\right) + G\cos\alpha - 2S\sin\alpha \end{Bmatrix} \quad (2)$$

Where u, v are the displacements of the rotor in the x, y directions, respectively; η is the oil viscosity; Ω is the speed of rotation of shaft; L, D, c are the bearing length, diameter, and radial clearance, respectively.

Thus, for the rotor - bearing system supported by a nonlinear bearing, equation of motion is:

$$M\ddot{q} + \Omega G\dot{q} + Kq = Q_b(q,\dot{q},t) + Q_{ub}(\Omega t) - Q_g \quad (3)$$

Where Q_b is a vector of bearing forces including the damping terms, Q_b is a vector of out-of-balance forces, and Q_g is a vector of gravitational forces. In equation (3):

$$\alpha = \tan^{-1}\left(\frac{v\Omega+2\dot{u}}{u\Omega-2\dot{v}}\right) - \frac{\pi}{2}\,\mathrm{sign}\left(\frac{v\Omega+2\dot{u}}{u\Omega-2\dot{v}}\right) - \frac{\pi}{2}\,\mathrm{sign}(v\Omega+2\dot{u}) \quad (4)$$

$$G(u,v,\alpha) = \frac{2c}{\sqrt{c^2-u^2-v^2}}\left\{\frac{\pi}{2} + \tan^{-1}\left(\frac{v\cos\alpha-u\sin\alpha}{\sqrt{c^2-u^2-v^2}}\right)\right\} \quad (5)$$

$$V(u,v,\alpha) = \frac{2c^2+c(v\cos\alpha-u\sin\alpha)G}{c^2-u^2-v^2} \quad (6)$$

$$S(u,v,\alpha) = \frac{c(u\cos\alpha+v\sin\alpha)}{c^2-(u\cos\alpha+v\sin\alpha)^2} \quad (7)$$

In this work, the parameters of the bearing are: L = 40 mm, D = 80 mm, c = 60 µm, η = 0,03 Pa.s.

3. RESULTS AND DISCUSTION

3.1. Comparison response of linear and nonlinear bearing

Figure 3 illustrates in the eccentricity between the rotor center and the bearing center with respect to rotor speed Ω. As the speed increases, the eccentricity decreases, leading to a change in the bearing force acting on the rotor. Figure 4 shows the orbits of the rotor center at Bearing 1 corresponding to the first six vibration modes. The cross denotes the start and the diamon denotes the end of the orbit. It can be observed that as the rotor speed increases, the influence of the hydrodynamic bearing force causes the rotor to become asymmetric, with the orbit transforming into an elliptical shape.

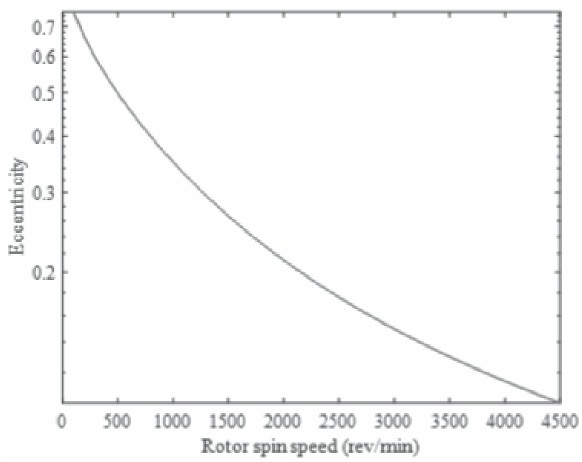

Figure 3. Eccentricity between the rotor center and the bearing center

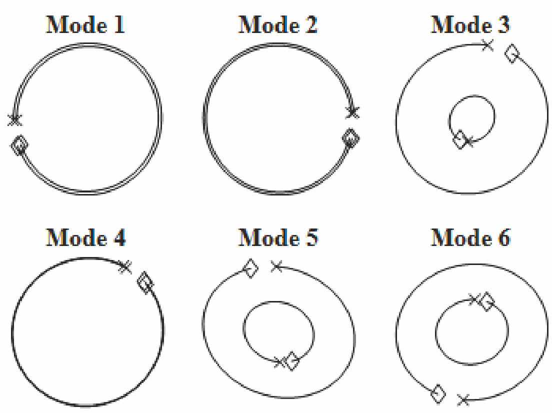

Figure 4. The axel view of the mode shape at bearing 1.

The Campbell diagram shows how rotor natural frequencies and excitation lines vary with rotor speed as shown in Figure 5. As speed increases, the forward whirl mode rises due to gyroscopic effects, while the backward mode drops. The 1X excitation line intersects the forward mode near 4000 rpm, indicating a potential resonance zone where oil whip may occur. Below this speed, the 0.5X line aligns with the forward mode, signaling the risk of oil whirl. These intersections highlight critical speeds where subsynchronous instabilities can arise. The second mode remains above all excitation lines, suggesting it's less likely to be excited. Overall, the diagram helps identify unsafe operating zones and the need for nonlinear modeling.

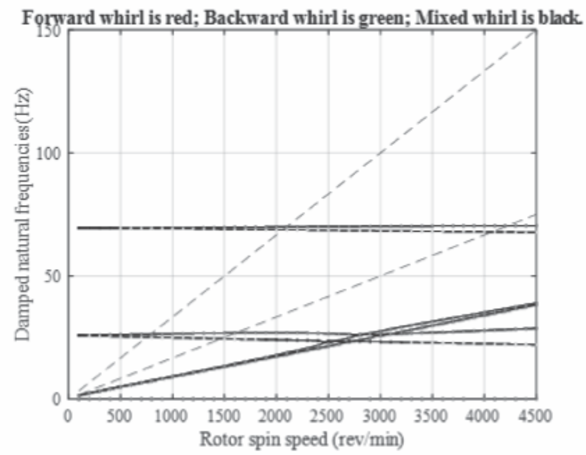

Figure 5. Campbel diagram

Time-domain simulations revealed critical differences between the linear and nonlinear bearing models shown in Figure 6. The linear model, the rotor response diverged rapidly at 4000 rpm, indicating instability. In contrast, the nonlinear bearing model stabilized into a limit-cycle oscillation. The vibration amplitude remained bounded, and a clear subsynchronous component emerged, corresponding to oil whirl behavior.

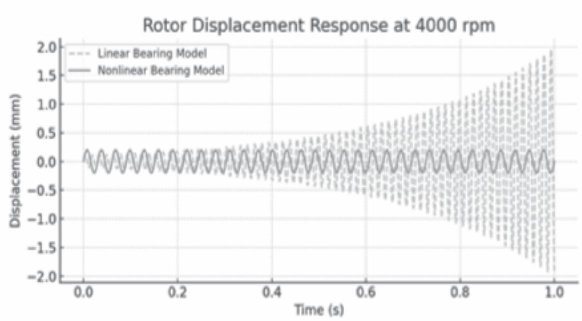

Figure 6. Rotor displacement response comparing linear and nonlinear bearing models

3.2. Oil Whirl and Oil Whip phenomena

The rotor orbits in the bearing clearance confirm the onset of oil whirl and whip phenomena as shown in Figure 7. At moderate speeds (< 4000 rpm), the rotor describes circular orbits at approximately 0.5X the rotation speed. This is a signature of whirl induced by cross-coupled stiffness of the hydrodynamic film. At or above 4000 rpm, the orbit pattern locks itnto the system's natural frequency (~22 Hz), and the whirl frequency becomes speed-independent. This reflects oil whip – a more severe instability where vibration can persist even as speed increases.

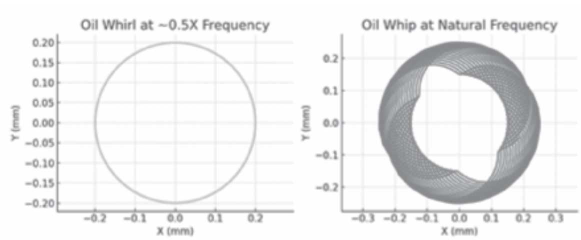

Figure 7. Orbit plots showing oil whirl and oil whip phenomena

A waterfall plot of frequency versus rotor speed highlights the transition from oil whirl to oil whip as shown in Figure 8. As speed increases: The 1X peak (synchronous) shifts proportionally with rotor speed. The 0.5X peak (subsynchronous) dominates at lower speeds and begins to fade near 4000 rpm. A flat, constant-frequency ridge at ~22 Hz emerges post-4000 rpm, confirming oil whip as the dominant vibration mode.

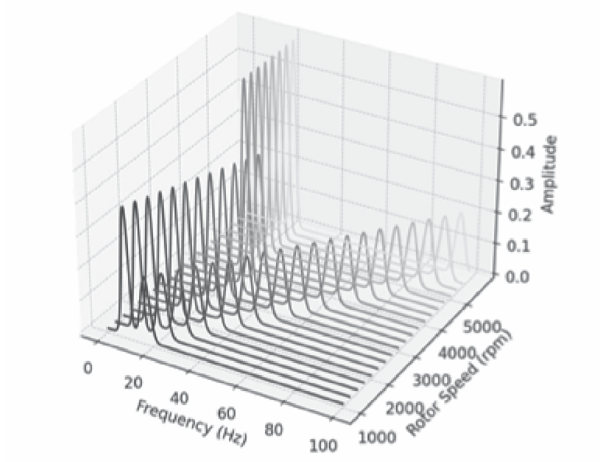

Figure 8. Waterfall plot at bearing 1.

A convenient method to determine stability is the root locus diagram, as shown in Figure 9. The system becomes unstable if any of the eigenvalues cross the imaginary axis and the real part becomes positive. It can be seen that, starting from 4,000 rpm, the rotor becomes unstable due to oil whip.

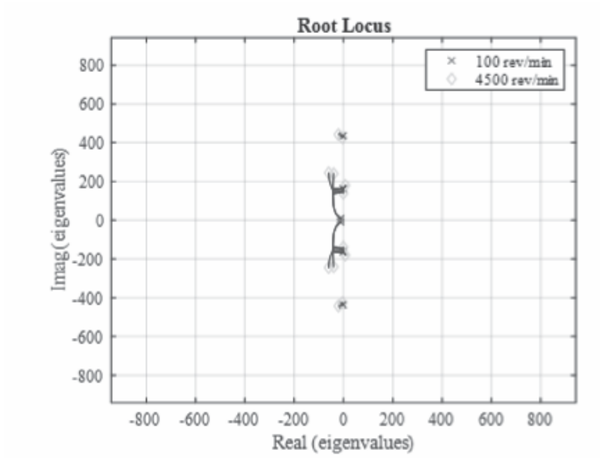

Figure 9. Root locus diagram

4. CONCLUSIONS

This study investigated the nonlinear dynamic behavior of a rotor system supported by hydrodynamic bearings. Finite element simulations revealed that gyroscopic effects induce mode splitting, while nonlinear bearing forces give rise to subsynchronous vibrations. Oil whirl was observed below 4000 rpm, with a transition to oil whip occurring near the first natural frequency. The nonlinear model predicted bounded limit-cycle behavior, unlike the divergent response of linear models. Orbit shapes and waterfall spectra confirmed the presence of oil-film-induced instabilities. These results highlight the need for nonlinear modeling to ensure accurate prediction and safe operation of high-speed rotating machinery.❖

References:

[1]. Ivanov, I. I., Belousov, V. V., Myasnikov, V. Y., Serebriakov, N. N., & Shadrin, D. V. (2020), "*Study of rotor dynamics considering a fluid film bearing*". In IOP Conference Series: Materials Science and Engineering (Vol. 747, No. 1, p. 012050). IOP Publishing.

[2]. Khamari, D. S., Kumar, J., & Behera, S. K. (2023), "*Rotordynamic analysis of a complex high-speed rotor*". Materials Today: Proceedings, 90, 299-304.

[3]. Yu, X., Shao, M., Yang, X., Lin, Y., Lan, Z., Li, L., ... & Jiang, H. (2025), "*Advances in the investigation of thermal characteristics of hydrostatic bearing spindle: an overview*". Journal of Thermal Analysis and Calorimetry, 1-33.

[4]. Smolík, L., Byrtus, M., Dyk, Š., & Hajžman, M. (2018), "*Dynamic behaviour of rotors supported by fluid-film bearings operated close to fluid-induced instability*". In MATEC Web of Conferences (Vol. 148, p. 04003). EDP Sciences.

[5]. Friswell, M. I. (2010), "*Dynamics of rotating machines*". Cambridge University Press.

[6]. Lee, G. Y., Park, M., & Ahn, K. (2025), "*Nonlinear vibration analysis of rotor systems with hydrodynamic journal bearings using harmonic balance method*". International Journal of Non-Linear Mechanics, 170, 104992.

[7]. Sun, W., Yan, Z., Tan, T., Zhao, D., & Luo, X. (2018), "*Nonlinear characterization of the rotor-bearing system with the oil-film and unbalance forces considering the effect of the oil-film temperature*". Nonlinear Dynamics, 92, 1119-1145.

[8]. Xia, Z., Qiao, G., Zheng, T., & Zhang, W. (2009), "*Nonlinear modeling and dynamic analysis of the rotor-bearing system*". Nonlinear Dynamics, 57, 559-577.

[9]. Jianping, J., Guang, M., Yi, S., & SongBo, X. (2004), "*On the non-linear dynamic behavior of a rotor – bearing system*". Journal of Sound and Vibration, 274(3-5), 1031-1044.

[10]. Zhao, Y., Zhu, Y. P., Lin, J., Han, Q., & Liu, Y. (2022), "*Analysis of nonlinear vibrations and health assessment of a bearing-rotor with rub-impact based on a data-driven approach*". Journal of Sound and Vibration, 534, 117068.